Journal of Asian Scientific Research
ISSN(e): 2223-1331
ISSN(p): 2226-5724
DOI: 10.18488/journal.2.2017.74.99.118
Vol. 7, No. 4, 99-118

URL: www.aessweb.com

NONLINEAR ANALYSIS OF FLEXIBLE FOUR LINKAGE MECHANISM

Ahmad Salah Edeen Nassef[1+]
Abdelfattah Abdelhamid[2]

[1,2]*Assistant Professor, Faculty of Engineering – Matria – Helwan University, Cairo, Egypt*

(+ Corresponding author)

Article History
Received: 20 April 2017
Revised: 23 May 2017
Accepted: 25 May 2017
Published: 30 May 2017

Keywords
Four linkage
Flexible
Lagrange equation
Finite element
Dynamic response.

ABSTRACT

This paper was discretizing numerically the links of the mechanism using finite element to develop model of unconstrained flexible mechanisms considering both axial and transverse deformations. The augmented Lagrange equations were used to drive the global governing equations. The equations of motion were solved for mechanisms with frequently varying mass, gyroscopic and stiffness matrices to compute the eigenvalues of the mechanism. The model of the mechanism was combination of flexible links connected by rotational pairs. The critical running speeds were calculated based on stability criterion method. The methods for determining critical operating speeds of linkage mechanisms with all links assumed as elastic members were applied in this work.

Contribution/ Originality: This study is one of very few studies which have investigated the equation of motion of flexible mechanism considering gyroscopic matrix in computing the eigenvalues of the mechanism.

1. INTRODUCTION

During last years, several researches discussed the problems of dynamic and stability of high speed flexible linkage system. The stability and dynamic response of high speed slider crank mechanism with uniform elastic connecting rod and a rigid crank were studied by Jasinski, et al. [1]. The Euler-Bernoulli and Timoshenko beams was considered to study the stability of a slider-crank mechanism by Badlani and Kleinhenz [2]. It was shown that new zones of instability appear when both rotary inertia and shear deformation were considered in the analysis. Liou and Erdman [3] stated that derivative from the principle of virtual displacement, a general finite element analysis of the flexible four bar linkage was developed a general finite element computer code. The perturbation method was used by Zhu and Chen [4] to investigate the dynamic stability of a connecting rod. Dynamic analysis of general planar linkage using a finite element approach was presented by Bahgat and Willmert [5]. The mechanism can be modeled as a set of links connected by rotating or translating pairs. The kineto-elastodynamic study was carried out using finite element method for high speed mechanisms by Nath and Ghosh [6].

Cleghorn, et al. [7] analyzed in detail a planar four-bar angular function generating mechanism. Maher, et al. [8] composed the domain of the displacements for the rigid and elastic components by discretizing domain into two

distinctive types of subdomains. The critical operating speeds were determined by Kalaycioglu and Bagci [9] based on the calculation of the natural frequencies of the considered type of free vibrations. Linkage mechanisms change their original geometries as a function of time during the cycle of kinematics motion. The analysis of the dynamic response of a completely elastic planar linkage was presented theoretically and experimentally by El-Hag [10].

Vasanti and Gupta [11]; Vasanti and Gupta [12] studied the dynamic stability of the practical four bars mechanism at various speeds in different regions considering damping. Equations of motion were derived by Nagarajan and David [13] using Lagrange's equation for elastic mechanism systems and solved using the finite element method. The dynamic stability of rigid four-bar and slider-crank mechanisms was studied by [14, 15]. The governing differential equation was obtained and transformed to a set of coupled Hill's equations by using Galerkin's method. The critical speeds ranges for an elastic mechanism were determined by Nagarajan and David [16].

Gasparetto [17] decomposed the motion of the mechanism into a rigid motion of a suitably defined ERLS (Equivalent Rigid Link Mechanisms) and an overlapped elastic motion. The equations of motion for the flexible mechanism were derived by applying of the virtual work principle. Integrated structural and control design of linkage mechanism for noise attenuation was studied by Xianmin, et al. [18]. Based on the integral of energy and numerical integration, a general algorithm was developed by Jazar [19]. The algorithm is then used to get parameters of a parametric equation to induce a periodic response.

The eigenvalues characterize the system stability. The stable linear system has no positive real part in eigenvalue. Furthermore, the asymptotically stable system has negative real parts (no zero real parts allowed) in eigenvalue. However, calculation all the eigenvalues of the state matrix of a system is not always desirable. In fact, computing the solution of the system is easier than calculation of the eigenvalue criteria, Inman [20].

2. EQUATION OF MOTION OF A MOVING LINK

Consider a flexible Link subject to translation and rotations of the rigid body shown in Figure (1). Also, consider a finite degrees of freedom are allowed as shown in Figure (2).

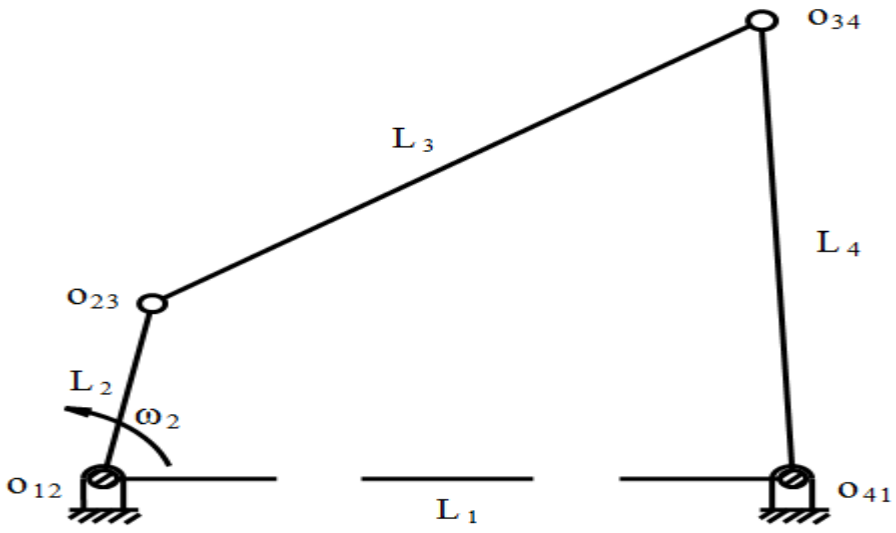

Figure-1. Configuration of a planer four-bar mechanism
Source: Autocad Drawing

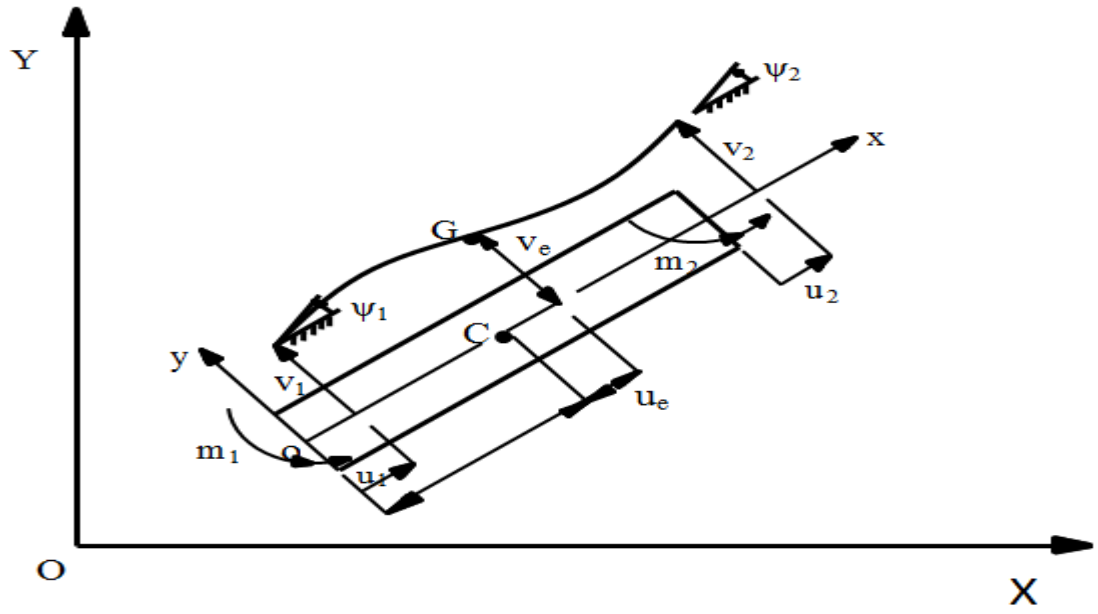

Figure-2. Deflection variables of flexible element

Source: Autocad Drawing

The considered link is referred to two frames of references, the global 'OXY' and the local 'oxy' frames. Rotations and deflections were represented by a quintic polynomial [7] as follows:

$$v_e = \sum_{i=0}^{5} C_i x^i \quad (1)$$

And the longitudinal deformations of the point "C" were presented by a linear polynomial as follows:

$$u_e = \sum_{j=6}^{7} C_j x^{j-6} \quad (2)$$

Where Cs are functions of time only, x is the distance measured from the left end of the element, as shown in Figure (2).

The end conditions are:

1 - At $x = 0$:

$$u_e = u_1, v_e = v_1, \frac{\partial v_e}{\partial x} = \psi_1 \text{ and } \frac{\partial^2 v_e}{\partial x^2} = m_1 \quad (3)$$

2 - At $x = L$:

$$u_e = u_2, v_e = v_2, \frac{\partial v_e}{\partial x} = \psi_2 \text{ and } \frac{\partial^2 v_e}{\partial x^2} = m_2 \quad (4)$$

By substituting in Equations (1), (2), the resulting equation can be expressed as follows:

$$\{C_v\}^T = \{\beta_v\}^T([D_v]^{-1})^T \quad (5)$$

and

$$\{C_u\}^T = \{\beta_u\}^T([D_u]^{-1})^T \quad (6)$$

Where:

$$\{C_v\}^T = [C_o \quad C_1 \quad C_2 \quad C_3 \quad C_4 \quad C_5]$$

$$\{\beta_v\}^T = [v_1\ \psi_1\ m_1\ v_2\ \psi_2\ m_2]$$

$$\{C_u\}^T = [C_6\quad C_7]$$

$$\{\beta_u\}^T = [u_1\quad u_2]$$

$$[D_v] = \begin{bmatrix} 1 & 0 & 0 & 0 & 0 & 0 \\ 0 & 1 & 0 & 0 & 0 & 0 \\ 0 & 0 & 2 & 0 & 0 & 0 \\ 1 & L & L^2 & L^3 & L^4 & L^5 \\ 0 & 1 & 2L & 3L^2 & 4L^3 & 5L^4 \\ 0 & 0 & 2 & 6L & 12L^2 & 20L^3 \end{bmatrix}$$

$$[D_v]^{-1} = \begin{bmatrix} 1 & 0 & 0 & 0 & 0 & 0 \\ 0 & 1 & 0 & 0 & 0 & 0 \\ 0 & 0 & \frac{1}{2} & 0 & 0 & 0 \\ -\frac{10}{L^3} & -\frac{6}{L^2} & -\frac{3}{2L} & \frac{10}{L^3} & -\frac{4}{L^2} & \frac{1}{2L} \\ \frac{15}{L^4} & \frac{8}{L^3} & \frac{3}{2L^2} & -\frac{15}{L^4} & \frac{7}{L^3} & -\frac{1}{L^2} \\ -\frac{6}{L^5} & -\frac{3}{L^4} & -\frac{1}{2L^3} & \frac{6}{L^5} & -\frac{3}{L^4} & \frac{1}{2L^3} \end{bmatrix}$$

$$[D_u] = \begin{bmatrix} 1 & 0 \\ 1 & L \end{bmatrix}$$

$$[D_u]^{-1} = \begin{bmatrix} 1 & 0 \\ -\frac{1}{L} & \frac{1}{L} \end{bmatrix}$$

From Equations (5) and (6), one can obtain:

$$\{C_v\} = \begin{bmatrix} v_1 \\ \theta_1 \\ m_1/2 \\ \frac{m_2}{2L} - \frac{3m_1}{2L} - \frac{4\theta_2}{L^2} - \frac{6\theta_1}{L^2} + 10v_2/L^3 - 10v_1/L^3 \\ -\frac{m_2}{L^2} + \frac{7\theta_2}{L^3} + \frac{8\theta_1}{L^3} + \frac{3m_1}{2L^2} - \frac{15v_2}{L^4} + 15v_1/L^4 \end{bmatrix} \quad (7)$$

$$\{C_u\} = \begin{bmatrix} u_1 \\ \frac{u_2 - u_1}{L} \end{bmatrix} \quad (8)$$

The transverse and longitudinal deflection can be expressed as:

$$v_e = \{\beta_v\}^T([D_v]^{-1})^T\{x_v\} \quad (9)$$

$$u_e = \{\beta_u\}^T([D_u]^{-1})^T\{x_u\} \quad (10)$$

Where:

$$\{x_v\} = [1 \quad x \quad x^2 \quad x^3 \quad x^4 \quad x^5]$$

$$\{x_u\} = [1 \quad x]$$

3. VELOCITY DISTRIBUTION OF FLEXIBLE TRANSLATING AND ROTATING LINK

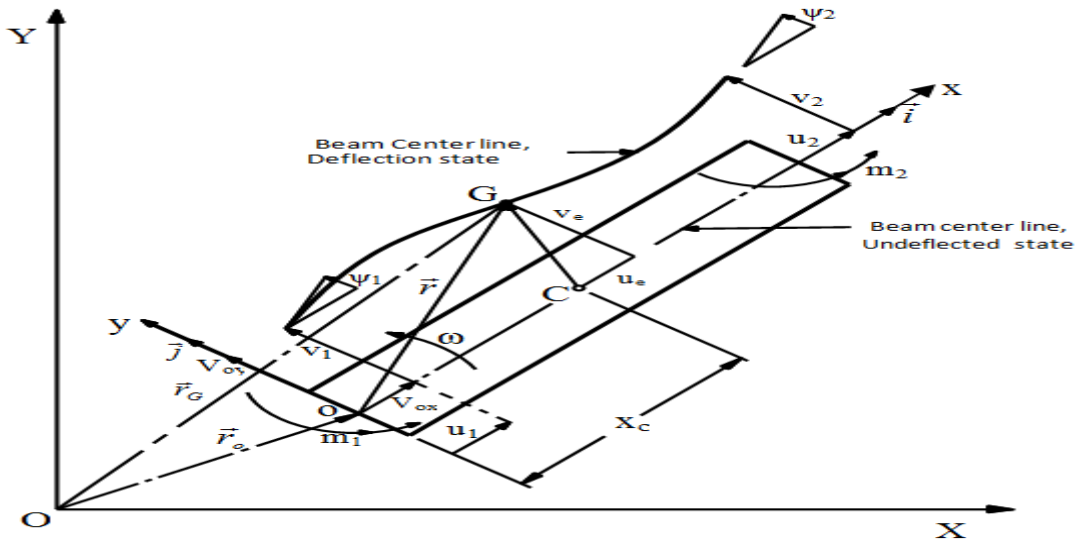

Figure-3. Position vector and velocity components of the finite beam element
Source: Autocad Drawing

The position vector of the point G, as shown in figure (3), is given by:

$$\overrightarrow{r_G} = \overrightarrow{r_o} + \vec{r} \tag{11}$$

Where:

$$\vec{r} = (x_C + u_e)\vec{i} + v_e\vec{j} \tag{12}$$

Differentiating Equation (11) with respect to time the velocity of point G can be given by:

$$\overrightarrow{v_G} = \overrightarrow{v_o} + \frac{d\vec{r}}{dt} \tag{13}$$

$$\overrightarrow{v_G} = \overrightarrow{v_o} + \Omega \times \vec{r} + \frac{d\vec{r}}{dt}\Big|_{\Omega=0} \tag{14}$$

Where:

$\overrightarrow{v_G}$ is the velocity vector of center point G.

$\overrightarrow{v_o}$ is the velocity vector of the point o.

$\Omega = \omega\vec{k}$ is the angular velocity of the beam element.

From equations (11) through (14), one can obtain that:

$$\overrightarrow{v_G} = \begin{bmatrix} \vec{i} & \vec{j} & \vec{k} \end{bmatrix} \begin{bmatrix} v_{ox} - v_e\omega + \dot{u}_e \\ v_{oy} + \omega(x_C + u_e) + \dot{v}_e \\ 0 \end{bmatrix} \quad (15)$$

4. KINETIC ENERGY OF FREE ROTATING BEAM ELEMENT

Let ρ be the mass per unit volume of element material, and A is the element cross sectional area, then the kinetic energy of the link is:

$$T_e = \frac{1}{2}\rho A \int_0^L \left[(v_{ox} - v_e\omega + \dot{u}_e)^2 + \left(v_{oy} + \omega(x_C + u_e) + \dot{v}_e\right)^2\right] dx \quad (16)$$

By differentiating Equations (9) and (10) with respect to time and substituting them into equation (16), one can obtain that:

$$T_e = T_1 + T_2 + T_3 + T_4 + T_5 + T_6 \quad (17)$$

Where:

$$T_1 = \frac{1}{2}\rho A \int_0^L [(\dot{u}_e)^2 + (\dot{v}_e)^2] dx \quad (18)$$

$$T_1 = \frac{1}{2}\{\dot{u}_e\}^T [M_e]\{\dot{u}_e\} \quad (19)$$

$[M_e]$: is the mass matrix (symmetric)

$$T_2 = \frac{1}{2}\rho A \int_0^L 2\omega[u_e - \dot{u}_e - \dot{v}_e + v_e] dx \quad (20)$$

$$T_2 = \frac{1}{2}\omega\{u_e\}^T [B_e]\{\dot{u}_e\} \quad (21)$$

$[B_e]$: Coriolis acceleration contribution matrix (skew-symmetric).

$$T_3 = \frac{1}{2}\rho A \int_0^L \omega^2[{u_e}^2 + {v_e}^2] dx \quad (22)$$

$$T_3 = \frac{1}{2}\omega^2\{u_e\}^T [M_e]\{u_e\} \quad (23)$$

$$T_4 = \frac{1}{2}\rho A \int_0^L 2\dot{v}_e(v_{oy} + \omega x + v_{ox}) dx \quad (24)$$

$$T_4 = \{\dot{u}_e\}^T\{Z_e\} \quad (25)$$

Where:

$$\{Z_e\} = \rho A(v_{oy}\{S_v\} + v_{ox}\{S_u\} + \omega\{W_v\}) \quad (26)$$

$$\{S_v\} = \int_0^L [N_v]^T [D_v]^T \{x\} dx \tag{27}$$

$$\{S_v\}^T = \begin{bmatrix} 0 & \frac{L}{2} & \frac{L^2}{10} & \frac{L^3}{120} & 0 & \frac{L}{2} & -\frac{L^2}{10} & \frac{L^3}{120} \end{bmatrix} \tag{28}$$

$$\{S_u\} = \int_0^L [N_u]^T ([D_u]^{-1})^T \{x\} dx \tag{29}$$

$$\{S_u\}^T = \begin{bmatrix} \frac{L}{2} & 0 & 0 & 0 & \frac{L}{2} & 0 & 0 & 0 \end{bmatrix} \tag{30}$$

$$\{W_v\} = \int_0^L x[N_v]^T ([D_v]^{-1})^T \{w\} dx \tag{31}$$

$$\{W_v\}^T = \begin{bmatrix} 0 & \frac{L^2}{7} & \frac{4L^3}{105} & \frac{L^4}{280} & 0 & \frac{5L^2}{14} & -\frac{13L^2}{210} & \frac{L^4}{210} \end{bmatrix} \tag{32}$$

$$T_5 = \frac{1}{2}\rho A \int_0^L \left(2\omega\left(v_{oy}u_e + xu_e - v_{ox}v_e\right)\right)^2 dx \tag{33}$$

$$T_5 = \{u_e\}^T \{Y_e\} \tag{34}$$

Where:

$$\{Y_e\} = \rho A\left(\omega^2\{W_u\} + v_{oy}\omega\{S_u\} + v_{oy}\omega\{s_v\}\right) \tag{35}$$

$$\{W_u\}^T = \begin{bmatrix} \frac{L^2}{6} & 0 & 0 & 0 & \frac{L^3}{3} & 0 & 0 & 0 \end{bmatrix} \tag{36}$$

and

$$T_6 = \frac{1}{2}\rho A\left(v_{oy}{}^2 L + v_{ox}{}^2 L + \frac{1}{3}\omega^2 L^3 + \omega L^2 v_{oy}\right) \tag{37}$$

5. STRAIN ENERGY OF THE FREE ROTATING BEAM ELEMENT

The strain energy due to elastic deformations of a uniform link with modulus of elasticity E and area moment of inertia I about neutral axis can be expressed as:

$$V_e = V_1 + V_2 + V_3 \tag{38}$$

$$V_e = \frac{EI}{2}\int_0^L \left(\frac{\partial^2 v_e}{\partial x^2}\right)^2 dx + \frac{EA}{2}\int_0^L \left(\frac{\partial u_e}{\partial x}\right)^2 dx + \frac{1}{2}\int_0^L P\left(\frac{\partial v_e}{\partial x}\right)^2 dx \tag{39}$$

Where:

V_1 is the flexural strain energy.

V_2 is the longitudinal strain energy.

V_3 is the strain energy due to longitudinal loads acting in an element undergoing transverse deflection.

P is the longitudinal rigid body inertia forces distributed on a moving beam element, as shown in Figure (4).

$$P = [P_R - \rho A(a_{ox}L - \omega^2 L^2/2)] + \rho A a_{ox} x - (\rho A \omega^2/2)\, x^2 \quad (40)$$

Where:

P_R is an external rigid body pin force.

a_{ox} is the acceleration of the point o in the x direction.

One can sum V_1 and V_2 to obtain V_s, where:

$$V_s = V_1 + V_2 = \{u_e\}^T [K_e]\{u_e\} \quad (41)$$

Where:

$[K_e]$ is as given in the appendix.

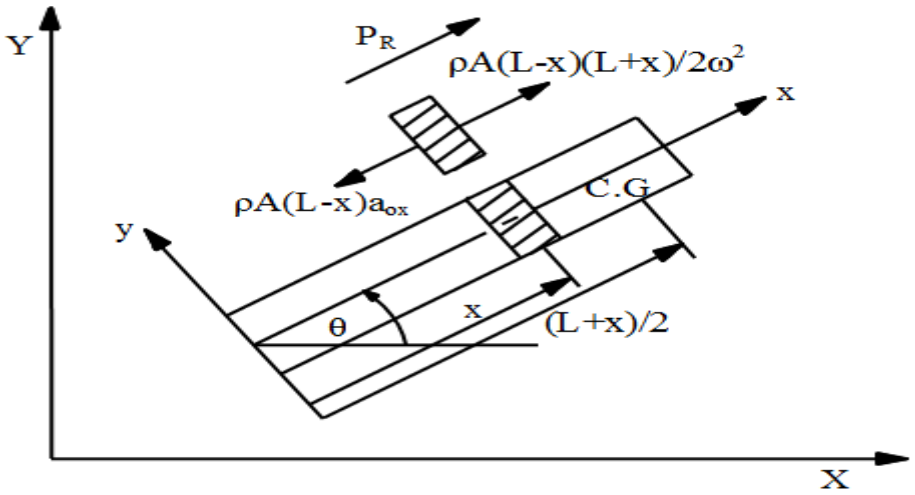

Figure-4. The longitudinal rigid body inertia forces distributed on a moving beam element
Source: Autocad Drawing

$$V_3 = \frac{1}{2}\{u_e\}(P_R - \rho A(a_{ox} L - \frac{1}{2}\omega^2 L^2)[A^*] + \rho A a_{ox}[B^*] - \frac{1}{2}\rho A \omega^2 [C^*])\{u_e\} \quad (42)$$

Where:

Matrices $[A^*]$, $[B^*]$ and $[C^*]$ are dimensional matrices, constant, symmetric and given in the appendix.

6. LAGRANGE EQUATIONS

The Lagrange for an arbitrarily translating and rotating flexible link is:

$$\frac{\partial L_e}{\partial \{u_e\}^T} - \frac{\mathrm{d}}{\mathrm{dt}}\left(\frac{\partial L_e}{\partial \{\dot{u}_e\}^T}\right) = \{0\} \quad (43)$$

Where:

L_e is the Lagrangian which is given by

$$L_e = T_e - V_e \tag{44}$$

Substituting Equations (39) and (16) in Equation (44), yields

$$\begin{aligned} L_e = {} & \frac{1}{2}\{\dot{u}_e\}^T[M_e]\{\dot{u}_e\} + \omega\{\dot{u}_e\}^T[B_e]\{u_e\} \\ & - \frac{1}{2}\{u_e\}^T[[K_e] + P_R[A^*] + \omega^2[D^*] + a_{ox}[E^*]]\{u_e\} \\ & + \{\dot{u}_e\}^T\{Z\} + \{u_e\}^T\{Y\} \\ & + \frac{\rho A}{2}(V_{ox}^2 L + V_{oy}^2 L + \frac{\omega^2 L^3}{6} + V_{oy} L^2 \omega). \end{aligned} \tag{45}$$

where

$$[D^*] = -[M_e] + (\rho A L^2)/2\,[A^*] - \rho A/2\,[C^*],$$

$$[E^*] = -\rho A L[A^*] + \rho A[B^*].$$

Matrices [D*] and [E*] are given in the appendix.

Substituting Equation (45) in Equation (43), one can obtain the governing equation for beam element in general motion:

$$[M_e]\{\ddot{u}_e\} + 2\omega[B_e]\{\dot{u}_e\} + ([Ke] + [K_d])\{u_e\} = \{P_e\} \tag{46}$$

Where:

$$\{P_e\} = \{Y_e\} - \{\dot{Z}_e\}.$$

$\{P_e\}$ is the element load vector.

$$[K_d] = \alpha[Be] + P_R[A^*] + \omega^2[D^*] + a_{ox}[E^*]$$

$[K_d]$ is the dynamic stiffness matrix.

7. TRANSFORM FROM LOCAL TO GLOBAL VARIABLES

The coordinates of every link are referred to the directions of the global variables, as shown in Figure (5).

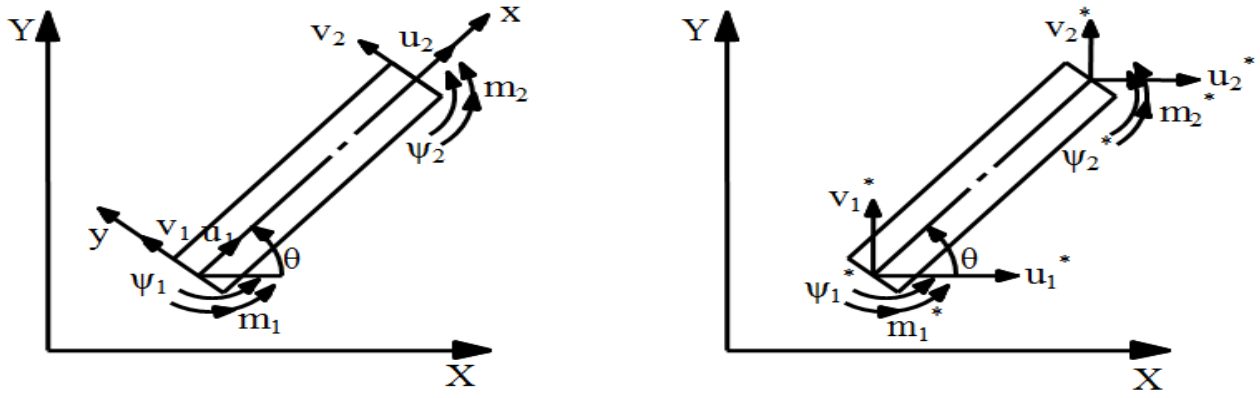

Figure-5. Transformation orientated from local to global coordinates

Source: Autocad Drawing

The set of variables can be put into a set of global variables as:

$$\{u_{e-g}\} = [u_1^* \; v_1^* \; \psi_1^* \; m_1^* \; u_2^* \; v_2^* \; \psi_2^* \; m_2^*]^T \tag{47}$$

The relation between local and global variables is given through the transformation matrix [R] such that:

$$\{u_e\} = [R]\{u_{e-g}\} \tag{48}$$

$$[R] = \begin{bmatrix} \cos\theta & \sin\theta & 0 & 0 & 0 & 0 & 0 & 0 \\ -\sin\theta & \cos\theta & 0 & 0 & 0 & 0 & 0 & 0 \\ 0 & 0 & 1 & 0 & 0 & 0 & 0 & 0 \\ 0 & 0 & 0 & 1 & 0 & 0 & 0 & 0 \\ 0 & 0 & 0 & 0 & \cos\theta & \sin\theta & 0 & 0 \\ 0 & 0 & 0 & 0 & -\sin\theta & \cos\theta & 0 & 0 \\ 0 & 0 & 0 & 0 & 0 & 0 & 1 & 0 \\ 0 & 0 & 0 & 0 & 0 & 0 & 0 & 1 \end{bmatrix} \tag{49}$$

The Lagrangian of the global system can be also expressed as:

$$L_{eT} = \sum_{i=1}^{N} L_{ei} \tag{50}$$

$$\begin{aligned} L_{eT} = \; & \sum_{i=1}^{N} \frac{1}{2}\left([R_i]^T\{u_{e-gi}\}^T\right)^{\cdot}[M_{ei}]\left([R_i]\{u_{e-gi}\}^T\right)^{\cdot} + \\ & \omega_i\left([R_i]\{u_{e-gi}\}^T\right)^{\cdot}[B_{ei}][R_i]\{u_{e-gi}\} - \frac{1}{2}[R_i]\{u_{e-gi}\}^T\left[[K_{ei}] + P_{Ri}\,[A_i^*] + \omega_i{}^2[D_i^*] + \right. \\ & \left. a_{oxi}\,[E_i^*]\right][R_i]\{u_{e-gi}\} + \left([R_i]^T\{u_{ei}\}^T\right)^{\cdot}\{Z_{ei}\} + [R_i]^T\{u_{e-gi}\}^T\{Y_{ei}\} \end{aligned} \tag{51}$$

Thus, the global equation of motion for N elements mechanism can be put in the form:

$$[M]\{\ddot{u}_{e-g}\} + [B]\{\dot{u}_{e-g}\} + [[Ks] + [Kd]]\{u_{e-g}\} = \{F\} \tag{52}$$

Where:

$$[M] = \sum_{i=1}^{N}[M_{e-gi}] \tag{53}$$

$$[M_{e-gi}] = [R_i]^T[M_{ei}][R_i] \tag{54}$$

$$[B] = \sum_{i=1}^{N}[B_{e-gi}] \tag{55}$$

$$[B_{e-gi}] = 2\omega_i[R_i]^T[B_{ei}][R_i] + 2[R_i]^T[M_{ei}][\dot{R}_i] \tag{56}$$

$$[K_S] = \sum_{i=1}^{N}[K_{e-gi}] \tag{57}$$

$$[K_{e-gi}] = [R_i]^T [K_{ei}][R_i] \quad (58)$$

$$[K_d] = \sum_{i=1}^{N} [K_{de-gi}] \quad (59)$$

$$[K_{d\,e-gi}] = [R_i]^T [K_{di}][R_i] + [R_i]^T [M_{ei}][\ddot{R}_i] + 2\omega_i [R_i][B_{ei}][\dot{R}_i] \quad (60)$$

$$\{F\} = \sum_{i=1}^{N} \{F_{e-gi}\} \quad (61)$$

$$\{F_{e-gi}\} = [R]^T \{P_{ei}\} \quad (62)$$

8. CRITICAL RUNNING SPEEDS

Predefining of the critical speeds increase efficiency and reduce computation time during the design process. Figure (6) shows comparison between the first four natural frequencies for theoretical presented model and experimental analysis of the dynamic response of a completely elastic planar linkage was presented by El-Hag [10].

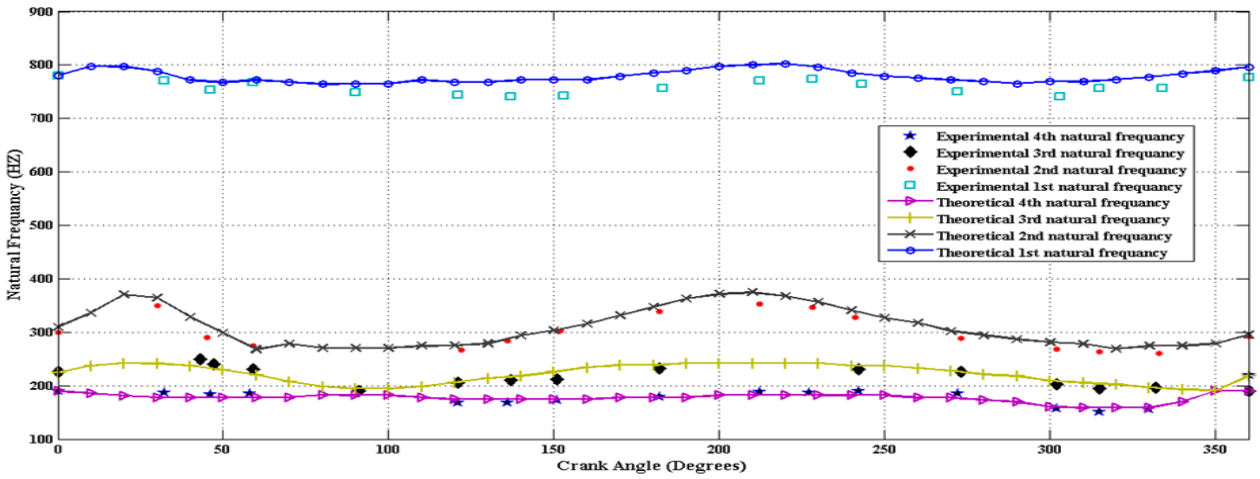

Figure-6. Comparison between the first four natural frequencies for theoretical and experimental works

Figure (6) shows a good agreement between the presented model and the experimental work of El-Hag [10]. Also it can be noted that the presented model is nearly approach to experimental work, which reflects the accuracy of the presented model.

The considered mechanism has thirty elastic degrees of freedom. The system matrices *[M], [B], [Kd]* and *[Ks]* are of order 30x30 and vectors $\{u\}$, $\{\dot{u}\}$ and $\{\ddot{u}\}$ are of length thirty. The engineering and geometrical properties of the elements of the mechanism are shown in Table (1).

The elastic displacements of the nodes that lie on the boundary between the input crank and the crank shaft are constrained to be zero. This boundary condition requires the base of the input crank to be given a known angular displacement as a function of time, which acts as the input to the system. Additionally, during the assembly of the link matrices to form the system matrices, the elastic degrees of freedom of nodes common to two or more links, are required to satisfy compatibility conditions, which ensure continuity in elastic motion at these nodes.

Table-1. Four bar mechanism parameters

Link / Properties	Crank (2)	Coupler (3)	Follower (4)
Area	107 mm^2	40.6 mm^2	40.6 mm^2
Link length	107.95 mm	279.2 mm	270.51 mm
Area moment of inertia	162 mm^4	8.67 mm^4	8.67 mm^4
Modulus of elasticity	71 GPa		
Weight density	$2.66*10^{-5}$ N/mm^3		
Distance between ground pivots = 254 mm			
Lamped mass of Bearing assembly = 0.42 N			

After decoupling the system equations, the natural frequencies ω for the different modes of vibration are obtained as functions in the mechanism positions, as shown in Figure (7).

The natural frequencies taking the gyroscopic ω_B are function in the mechanism positions and in the angular speeds of input link, are shown in Figure (8) and Figure (9). This natural frequencies ω and ω_B function for a particular mode of vibration are then used to obtain the monodromy matrix, for that mode of vibration and for a given speed of operation. The stability characteristics of the system at that operating speed is based on the eigenvalues of the monodromy matrix as per Floquet theory. This procedure can be carried out for all the desired number of modes of vibration.

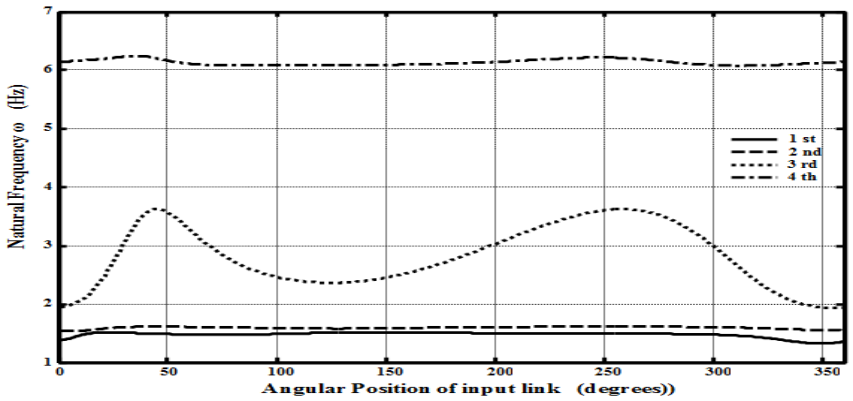

Figure-7. Variation of first four natural frequencies 'ω' throughout one cycle of crank rotation.

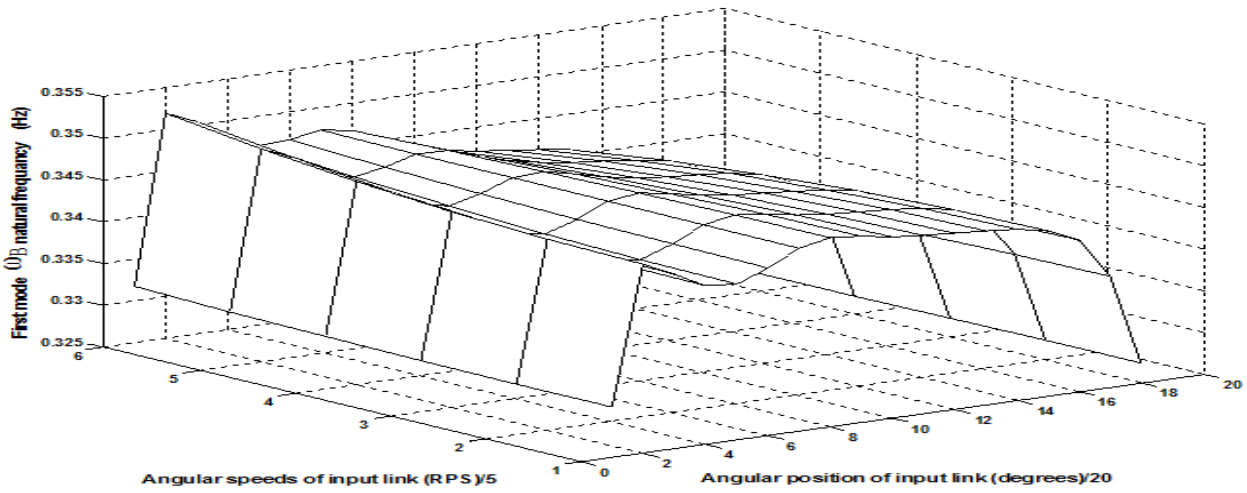

Figure-8. Variation of the first natural frequency ω_B throughout angular position and angular operating speeds

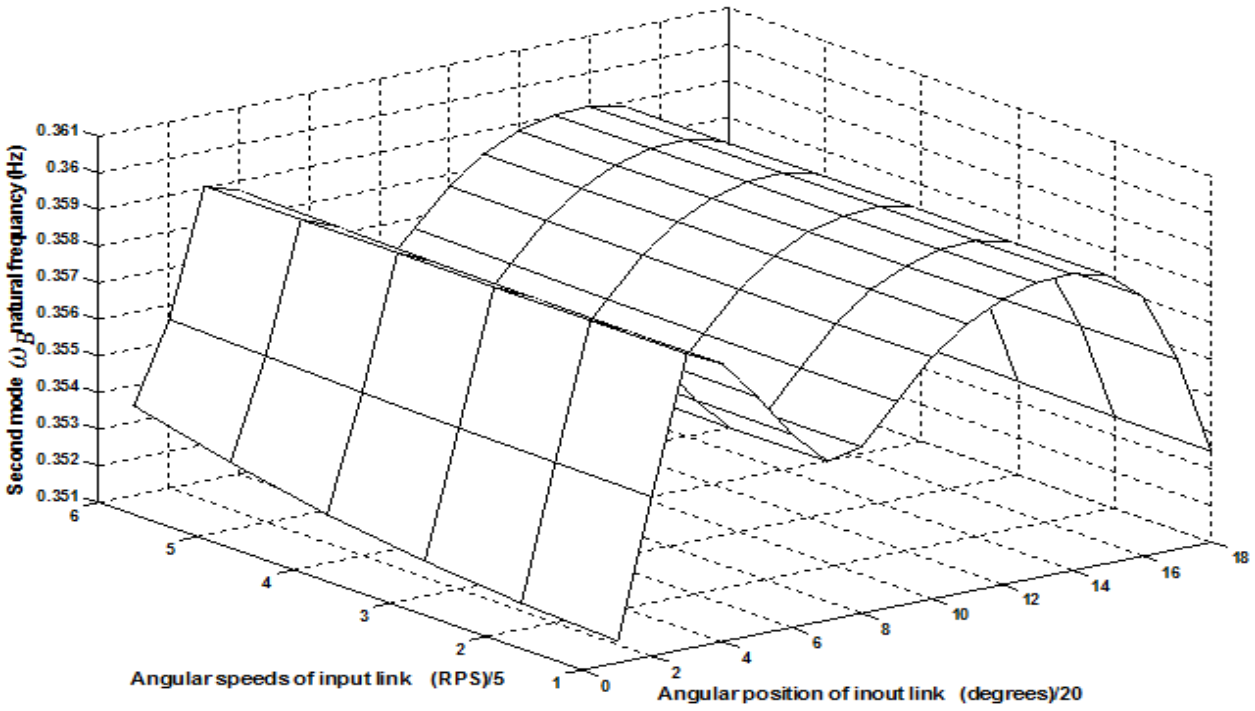

Figure-9. Variation of the second natural frequency ω_B throughout angular position and angular operating speeds

In addition, the stable and unstable boundaries for elastic linkage of four bar mechanism considering the mass matrix $[M]$ and static stiffness matrix $[K_s]$ only, as shown in Figure (10).

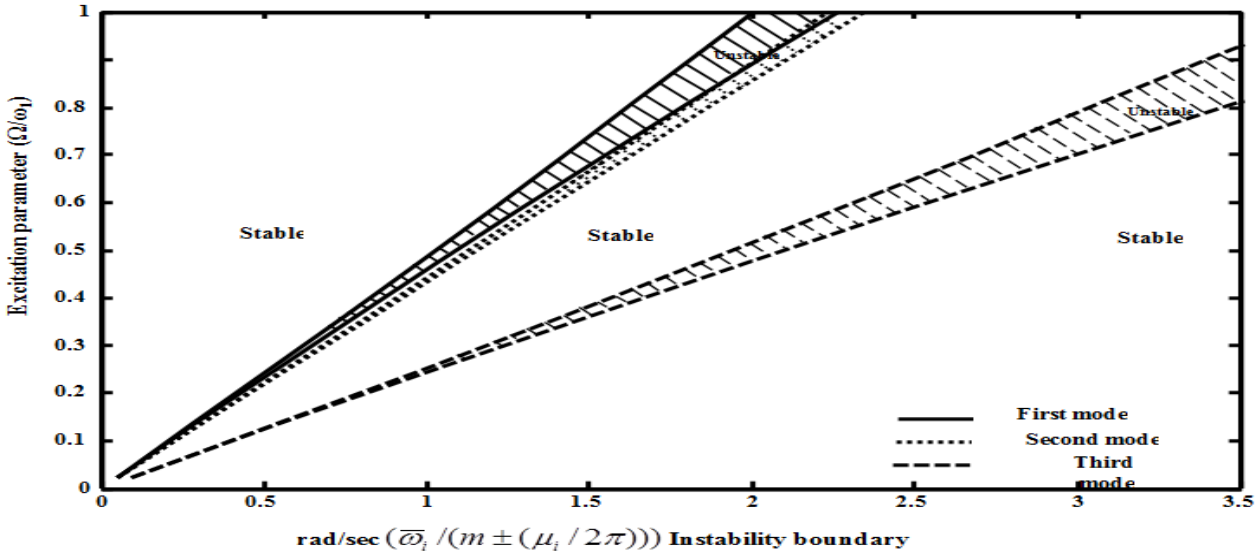

Figure-10. Excitation parameter Ω/ω1 as a function of instability boundary zones ($[M]$ and $[Ks]$ are considered)

The area of instability in Figure (10) is small because the effect of input link speeds is not considered in this case of study and the area of instability by second mode is very small because the variation of second mode of natural frequency with angular position of input link is very small as in Figure (7).

In Figure (11), the unstable areas are markedly larger than the unstable areas in Figure (10) as the dynamic stiffness matrix $[K_d]$ has been considered with $[M]$ and $[K_s]$ where $[K_d]$ serves as a function with angular speed of input link .

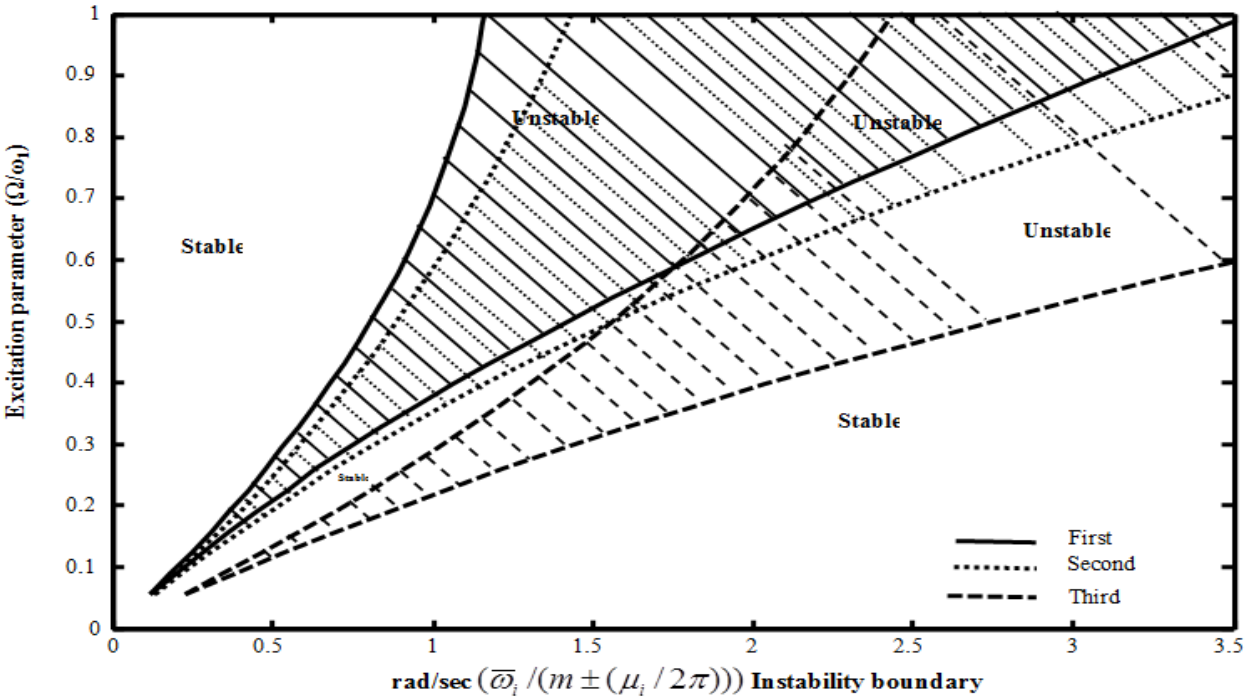

Figure-11. Excitation parameter Ω/ω_1 as a function of instability boundary zones ([M], [K_t] and [K_d] are considered)

Figure (12) shows the effect of gyroscopic parameter on the dynamic stability. This parameter causes an increase in the range of the stability areas at low operating speeds as well as the range of the instability areas at high operating speeds.

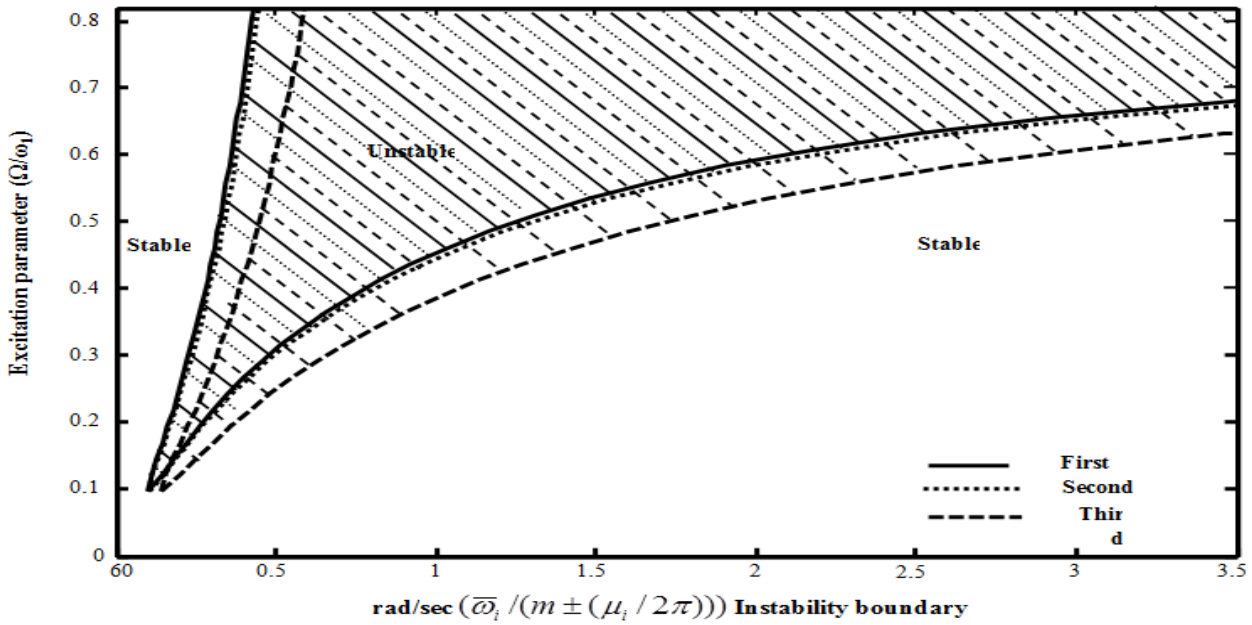

Figure-12. Excitation parameter Ω/ω_1 as a function of instability boundary zones ([M], [K_t], [K_d] and [B] are considered)

9. CONCLUSION

The finite element method is used to simulate the flexible mechanism. The equation of motion of flexible mechanisms has been derived using Lagrange equations. The method is applied to study the gyroscopic effect.

Considering gyroscopic effect gives a good results and agreement with experimental results. A comparison of the three stability charts gives a clear idea on the gyroscopic effect for an elastic linkage mechanism. The instability

bands are narrow in the absence of gyroscopic effect. The presence of gyroscopic effect yields wider instability bands. Finally, gyroscopic effect causes a decrease in the instability areas at low operating speeds.

NOTATIONS

A	Cross section area
$[B_e]$	Gyroscopic element matrix
$[B]$	Total global gyroscopic matrix
C_i	Constants
E	Modulus of elasticity
$[7]$	Global load vector for mechanism
$\{F_{e-g}\}$	Global load vector for link
I	Second moment of area
$[K_d]$	Dynamic stiffness matrix
$[K_s]$	Static stiffness matrix
$[K]$	Global overall stiffness matrix
L	Element length
L	Lagrange of global system
$[M]$	Global overall mass matrix
m	Curvature
T_e	Kinetic energy
t	Time
P_R	External rigid body pin force
$[R]$	Transformation matrix
u_e	Axial displacement
v_e	Transverse deformation
V_e	Strain energy
α_i	Angular accelerations for i link
ρ	Density
ψ	Slope
Ω	Forced frequency
ω	Natural frequency without gyroscopic effect
ω_B	Natural frequency with gyroscopic effect
ω_i	Angular velocity for i link

Funding: This study received no specific financial support.
Competing Interests: The authors declare that they have no competing interests.
Contributors/Acknowledgement: Both authors contributed equally to the conception and design of the study.

REFERENCES

[1] P. W. Jasinski, H. C. Lee, and G. N. Sandor, "Stability and steady state vibrations in a high speed slider crank mechanism," *Applied Mechanics*, vol. 37, pp. 1069-1076, 1970. *View at Google Scholar | View at Publisher*

[2] M. Badlani and W. Kleinhenz, "Dynamic stability of elastic mechanisms," *Mechanical Design*, vol. 101, pp. 149-153, 1979. View at Publisher

[3] W. Liou and A. G. Erdman, "Analysis of high speed flexible four bar linkage: Part I – Formulation and solution," *Journal of Vibration, Acoustics, Stress, and Reliability in Design*, vol. 111, pp. 35-41, 1989. View at Google Scholar | View at Publisher

[4] G. Zhu and Y. Chen, "The stability of the motion of a connecting rod," *Mechanism Transmissions and Automation in Design*, vol. 105, pp. 637-640, 1983. View at Google Scholar | View at Publisher

[5] B. M. Bahgat and K. D. Willmert, "Finite element vibrational analysis of planar mechanisms," *Mechanism and Machine Theory*, vol. 11, pp. 47- 71, 1976. View at Google Scholar | View at Publisher

[6] P. K. Nath and A. Ghosh, "Kinto-Elastodynamic analysis of mechanisms by finite element method," *Mechanism and Machine Theory*, vol. 15, pp. 179-197, 1980. View at Google Scholar | View at Publisher

[7] W. L. Cleghorn, R. G. Fenton, and B. Tabarrok, "Finite element analysis of high speed flexible mechanism," *Mechanism and Machine Theory*, vol. 16, pp. 407-424, 1981. View at Google Scholar | View at Publisher

[8] A. Maher, P. G. Kessel, and R. D. Cook, "A partitioned finite element method for dynamic systems," *Computers and Structures*, vol. 18, pp. 81-91, 1984. View at Google Scholar | View at Publisher

[9] S. Kalaycioglu and C. Bagci, "Determination of critical operating speeds of planar mechanism by the finite element method using planar actual line element and lumped mass systems," *Transactions of ASME*, vol. 101, pp. 210-223, 1979. View at Google Scholar | View at Publisher

[10] H. A. E.-D. El-Hag, "Elastodynamic analysis of planar linkages," Ph. D. Dissertation, Helwan University, 1987.

[11] M. Vasanti and K. N. Gupta, "Stability analysis of four bar mechanism part I with the assumption that damping is absent," *Mechanism and Machine Theory* vol. 23, pp. 367-375, 1988. View at Google Scholar | View at Publisher

[12] M. Vasanti and K. N. Gupta, "Stability analysis of four bar mechanism part II taking damping into consideration," *Mechanism and Machine Theory*, vol. 23, pp. 377-382, 1988. View at Google Scholar | View at Publisher

[13] S. Nagarajan and A. T. David, "Lagrangian formulation of the equations of motion for elastic mechanisms with mutual dependence between rigid body and elastic motions," *Part I: Element Level Equations, Dynamic Systems, Measurement, and Control*, vol. 112, pp. 203-214, 1990. View at Google Scholar | View at Publisher

[14] Ö. Turhan, "Dynamic stability of four bar and slider crank mechanism with elastic coupler," *Mechanism and Machine Theory*, vol. 36, pp. 871- 882, 1995. View at Google Scholar | View at Publisher

[15] Ö. Turhan, "Dynamic stability of four bar and slider crank mechanism with viscoelastic (Kelvin voigt model) coupler," *Mechanism and Machine Theory*, vol. 31, pp. 77-89, 1996. View at Google Scholar | View at Publisher

[16] S. Nagarajan and A. T. David, "General methods of determining stability and critical speeds for elastic mechanism systems," *Mechanism and Machine Theory*, vol. 25, pp. 209-223, 1990. View at Google Scholar | View at Publisher

[17] A. Gasparetto, "Accurate modeling of a flexible link planar mechanism by means of a linearized model in the state space form for design of a vibration controller," *Journal of Sound and Vibration*, vol. 240, pp. 241-262, 2001. View at Google Scholar | View at Publisher

[18] Z. Xianmin, J. Lu, and Y. Shen, "Simultaneous optimal structure and control design of flexible linkage mechanism for noise attenuation," *Sound and Vibration*, vol. 299, pp. 1124-1133, 2007. View at Google Scholar | View at Publisher

[19] N. G. Jazar, "Stability chart of parametric vibrating systems using energy-rate method," *International Journal of Non-Linear Mechanics*, vol. 39, pp. 1319 – 1331, 2004. View at Google Scholar | View at Publisher

[20] D. J. Inman, "Stability, in vibration with control," ed. Chichester, UK: John Wiley & Sons, Ltd, 2006.

Appendix

Listed this appendix are load vector and matrices associated with the governing equation of an element.

$$[7] = \rho A \begin{bmatrix} \frac{-a_{ox}L}{2} + \frac{\dot{\gamma}^2 L^2}{6} \\ \frac{-a_{oy}L}{2} - \frac{\ddot{\gamma} L^2}{7} \\ \frac{-a_{oy}L^2}{10} - \frac{4\ddot{\gamma} L^3}{105} \\ \frac{a_{oy}L^3}{120} - \frac{\ddot{\gamma} L^4}{280} \\ \frac{-a_{ox}L}{2} + \frac{\dot{\gamma}^2 L^2}{3} \\ \frac{-a_{oy}L}{2} - \frac{5\ddot{\gamma} L^2}{14} \\ \frac{a_{oy}L^2}{10} + \frac{13\ddot{\gamma} L^3}{210} \\ \frac{-a_{oy}L^3}{120} - \frac{\ddot{\gamma} L^4}{210} \end{bmatrix} \quad (1)$$

Where a_{ox} and a_{oy} are the absolute acceleration components of point o in the *x-y* coordinate system, which can also be expressed as

$$a_{ox} = \dot{V}_{ox} - \dot{\gamma} V_{oy}. \quad (2)$$

$$a_{oy} = \dot{V}_{oy} + \dot{\gamma} V_{ox}. \quad (3)$$

$$[M_e] = \rho A \begin{bmatrix} \frac{L}{3} & 0 & 0 & 0 & \frac{L}{6} & 0 & 0 & 0 \\ & \frac{181L}{462} & \frac{311L^2}{4620} & \frac{281L^3}{55440} & 0 & \frac{25L}{231} & \frac{-151L^2}{4620} & \frac{181L^3}{55440} \\ & & \frac{52L^3}{3465} & \frac{23L^4}{18480} & 0 & \frac{151L^2}{4620} & \frac{-19L^3}{1980} & \frac{13L^4}{13860} \\ & & & \frac{L^5}{9240} & 0 & \frac{181L^3}{55440} & \frac{-13L^4}{13860} & \frac{L^5}{11088} \\ & & & & \frac{L}{3} & 0 & 0 & 0 \\ & & \textit{Symmetric} & & & \frac{181L}{462} & \frac{-311L^2}{4620} & \frac{281L^3}{55440} \\ & & & & & & \frac{52L^3}{3465} & \frac{-23L^4}{18480} \\ & & & & & & & \frac{L^5}{9240} \end{bmatrix} \quad (4).$$

$$[B_e] = \rho A \begin{bmatrix} 0 & \frac{-5L}{14} & \frac{-13L^2}{210} & \frac{-L^3}{210} & 0 & \frac{-L}{7} & \frac{4L^2}{105} & \frac{-L^3}{280} \\ & 0 & 0 & 0 & \frac{L}{7} & 0 & 0 & 0 \\ & & 0 & 0 & \frac{4L^2}{105} & 0 & 0 & 0 \\ & & & 0 & \frac{L^3}{280} & 0 & 0 & 0 \\ & & & & 0 & \frac{-5L}{14} & \frac{13L^2}{210} & \frac{-L^3}{210} \\ & Skew- & Symmetric & & & 0 & 0 & 0 \\ & & & & & & 0 & 0 \\ & & & & & & & 0 \end{bmatrix} \quad (5).$$

$$[K_e] = EI \begin{bmatrix} \frac{EA}{L} & 0 & 0 & 0 & \frac{-EA}{L} & 0 & 0 & 0 \\ & \frac{120EI}{7L^3} & \frac{60EI}{7L^2} & \frac{3EI}{7L} & 0 & \frac{-120EI}{7L^3} & \frac{60EI}{7L^2} & \frac{-3EI}{7L} \\ & & \frac{192EI}{35L} & \frac{22EI}{70} & 0 & \frac{-60EI}{7L^2} & \frac{108EI}{35L} & \frac{-4EI}{35} \\ & & & \frac{6EIL}{70} & 0 & \frac{-3EI}{7L} & \frac{4EI}{35} & \frac{EIL}{70} \\ & & & & \frac{EA}{L} & 0 & 0 & 0 \\ & Symmetric & & & & \frac{120EI}{7L^3} & \frac{-60EI}{7L^3} & \frac{3EI}{7L} \\ & & & & & & \frac{192EI}{23L} & \frac{-22EI}{70} \\ & & & & & & & \frac{6EIL}{70} \end{bmatrix} \quad (6).$$

$$[A^*] = \begin{bmatrix} 0 & 0 & 0 & 0 & 0 & 0 & 0 & 0 \\ & \frac{10}{7L} & \frac{3}{14} & \frac{L}{84} & 0 & \frac{-10}{7L} & \frac{3}{14} & \frac{-L}{84} \\ & & \frac{8L}{35} & \frac{L^2}{60} & 0 & \frac{-3}{14} & \frac{-L}{70} & \frac{L^2}{210} \\ & & & \frac{L^3}{630} & 0 & \frac{-L}{84} & \frac{-L^2}{210} & \frac{L^3}{1260} \\ & & & & 0 & 0 & 0 & 0 \\ & Symmetric & & & & \frac{10}{7L} & \frac{-3}{14} & \frac{L}{84} \\ & & & & & & \frac{8L}{35} & \frac{-L^2}{60} \\ & & & & & & & \frac{L^3}{630} \end{bmatrix} \quad (7).$$

$$[B^*]=\begin{bmatrix} 0 & 0 & 0 & 0 & 0 & 0 & 0 & 0 \\ & \frac{5}{7} & \frac{13L}{84} & \frac{L^2}{84} & 0 & \frac{-5}{7} & \frac{5L}{84} & 0 \\ & & \frac{13L^2}{210} & \frac{29L^3}{5040} & 0 & \frac{-13L}{84} & \frac{-L^2}{140} & \frac{13L^3}{5040} \\ & & & \frac{L^4}{1680} & 0 & \frac{-L^2}{84} & \frac{-11L^3}{5040} & \frac{L^4}{2520} \\ & & & & 0 & 0 & 0 & 0 \\ & & & & & \frac{5}{7} & \frac{-5L}{84} & 0 \\ & & & & & & \frac{L^2}{6} & \frac{-11L^3}{1008} \\ & & & & & & & \frac{L^4}{1008} \end{bmatrix} \quad (8).$$

Symmetric

$$[C^*]=\begin{bmatrix} 0 & 0 & 0 & 0 & 0 & 0 & 0 & 0 \\ & \frac{30L}{77} & \frac{23L^2}{231} & \frac{2L^3}{231} & 0 & \frac{-30L}{77} & \frac{L^2}{231} & \frac{L^3}{308} \\ & & \frac{16L^3}{495} & \frac{29L^4}{9240} & 0 & \frac{-23L^2}{231} & \frac{-31L^3}{3465} & \frac{L^4}{495} \\ & & & \frac{L^5}{3080} & 0 & \frac{-2L^3}{231} & \frac{-L^4}{616} & \frac{L^5}{3696} \\ & & & & 0 & 0 & 0 & 0 \\ & & & & & \frac{30L}{77} & \frac{-L^2}{231} & \frac{-L^3}{308} \\ & & & & & & \frac{95L^3}{693} & \frac{-23L^3}{2772} \\ & & & & & & & \frac{L^5}{1386} \end{bmatrix} \quad (9).$$

Symmetric

$$[D^*] = \rho A \begin{bmatrix} \frac{-L}{3} & 0 & 0 & 0 & \frac{-L}{6} & 0 & 0 & 0 \\ & \frac{59L}{462} & \frac{-23L^2}{2310} & \frac{-191L^3}{55440} & 0 & \frac{-145L}{231} & \frac{53L^2}{385} & \frac{-601L^3}{55440} \\ & & \frac{32L^3}{385} & \frac{17L^4}{3080} & 0 & \frac{-104L^2}{1155} & \frac{8L^3}{1155} & \frac{L^4}{2310} \\ & & & \frac{29L^5}{55440} & 0 & \frac{-271L^3}{55440} & \frac{-L^4}{1584} & \frac{19L^5}{110880} \\ & & & & \frac{-L}{3} & 0 & 0 & 0 \\ & & & & & \frac{59L}{462} & \frac{-29L^2}{770} & \frac{139L^3}{55440} \\ & & & & & & \frac{71L^3}{2310} & \frac{-163L^4}{55440} \\ & & & & & & & \frac{L^5}{3080} \end{bmatrix}$$

(10).

Symmetric

$$[\mathbf{E}^{*}] = \rho A \begin{bmatrix} 0 & 0 & 0 & 0 & 0 & 0 & 0 & 0 \\ & \frac{-5}{7} & \frac{-5L}{84} & 0 & 0 & \frac{5}{7} & \frac{-13L}{84} & \frac{L^2}{84} \\ & & \frac{-L^2}{6} & \frac{-11L^3}{1008} & 0 & \frac{5L}{84} & \frac{L^2}{140} & \frac{-11L^3}{5040} \\ & & & \frac{-L^4}{1008} & 0 & 0 & \frac{13L^3}{5040} & \frac{-L^4}{2520} \\ & & & & 0 & 0 & 0 & 0 \\ & & Symmetric & & & \frac{-5}{7} & \frac{13L}{84} & \frac{-L^2}{84} \\ & & & & & & \frac{-13L^2}{210} & \frac{29L^3}{5040} \\ & & & & & & & \frac{-L^4}{1680} \end{bmatrix}$$

(11).